FRI-9.3-1-THPE-10

NUMERICAL STUDY OF THE FLOW PASSING THROUGH THE ROTOR OF A VERTICAL AXIS WIND TURBINE

Ahmed Ahmedov, PhD
Department of Thermotechnics, Hydraulics and Ecology,
"Angel Kanchev" University of Ruse, Ruse
Phone: +359 883 34 84 32
E-mail: aahmedov@uni-ruse.bg, aahmedov086@gmail.com

Milen Venev, PhD
Department of Thermotechnics, Hydraulics and Ecology,
"Angel Kanchev" University of Ruse, Ruse
Phone: +359 883 33 34 25
E-mail: m_venev@abv.bg

Assoc. Prof. Krasimir Tujarov, PhD
Department of Thermotechnics, Hydraulics and Ecology,
"Angel Kanchev" University of Ruse, Ruse
Phone: +359 885 59 72 30
E-mail: tujarov@uni-ruse.bg

Abstract: *A Savonius type wind turbine is the subject of the present study. The Savonius wind turbine has a relatively simple design, omnidirectional wind acceptance, excellent self-starting capabilities and stable operation under turbulent wind. The operation of the Savonius wind turbine is characterized by pronounced unsteadiness, due to the continuous change of the relative velocity acting on the blades. In order to gain deeper understanding over the ongoing processes during the turbine operation a numerical modelling of the flow passing through its rotor was carried out. Due to computational hardware and time limitations a 2D URANS approach was adopted. The k-ω SST turbulence model was chosen for the calculation of the vortex structures generation, dissipation and interactions. The k-ω SST combines the advantage of the k-ε model of excellent main flow modelling and the advantage of the k-ω model of excellent near-wall (blades) flow modelling. The obtained numerical data was postprocessed and the flow passing through the rotor was visualized at different angular positions. The aerodynamic theoretical characteristics of the Savonius wind turbine are obtained.*

Keywords: *Numerical Modelling, ANSYS Fluent, VAWT, Vortex Structures, Theoretical Aerodynamic Characteristics.*

INTRODUCTION

The classical Savonius wind turbine is a vertical axis wind turbine (VAWT) comprised by two semicircular blades which are displaced relative to the rotor axis of rotation. The blades are mounted between two end plates. The operational principal of the Savonius wind rotor is the Drag Force principal. This principal depicts the difference between the aerodynamic drag forces acting on the turbine blades surfaces as its main mechanism for generation of an active torque.

The Computational Fluid Dynamics (CFD) is an attractive approach for aerodynamic modeling of the operation of different types of wind turbines. Based on the numerical modeling results the theoretical operational characteristics can be obtained. The adequate physical modeling of the force interaction between a rotating wind turbine and the main flow is achieved through the implementation of the Sliding Mesh technique.

The standard $k - \varepsilon$ [6] turbulent model is the most widely used model for theoretical investigations of a broad specter of industrial and commercial problems. The $k - \varepsilon$ model is best suited for problems which involves fully developed turbulent flows. In most cases the obtained theoretical results are close to the experimental data, as opposed to the results obtained by the

Spalart-Allmaras turbulent model [10].

The $k - \omega \, SST$ is a two equations turbulent model, which combines the excellent modeling of the main flow provided by the $k - \varepsilon$ model and the reliable near wall modeling of the flow provided by the $k - \omega$ model [8, 7].

By incorporating the $k - \omega \, SST$ model, Abraham et al. [1] carried out an 2D numerical modeling over the performance of a Savonius wind turbine. The comparison between the theoretical results and the experimental data showed that the shape of the theoretical operational curve is in good correlation with the experimental one. But the values of the theoretical operational points are overestimating the experimental ones.

Plourde et al. [9] carried out an 3D $k - \omega \, SST$ modeling over the operation of a Savonius rotor. The researchers found that there is a very good correlation between the theoretical and experimental data.

Jaohindy et al. [5] conducted an 3D numerical investigation over the performance of a single stage Savonius wind rotor. The RANS approach was adopted in combination with the $k - \varepsilon$ and $k - \omega \, SST$ turbulence models. The comparison of the results showed that the $k - \omega \, SST$ model provides results which are closer to the experimental data.

On basis of the presented literature review regarding the numerical modeling of the operation of VAWT Savonius type it can be concluded that the $k - \omega \, SST$ turbulence model is suitable for theoretical analysis of the prominent unsteady nature of VAWT operational regimes.

The main objectives of the present study are the visualization of the flow passing through a single stage, double bladed Savonius wind rotor and the theoretical aerodynamic characteristics $C_m = f(\lambda)$, $C_P = f(\lambda)$ creation, where λ is the rotor tip speed ratio (TSR), C_m is the torque coefficient and C_P is the power coefficient.

In order to accomplish the objectives of the present study the following tasks are formed: Numerical modeling of the operation of a VAWT Savonius type through the aid of CFD software; Simulation of the turbine operation at different operational regimes; Visualization of the flow field at two different operational regimes; creation of the theoretical aerodynamic characteristics.

EXPOSITION

Numerical modeling procedure

The subject of the present study is a classical Savonius wind rotor comprise by two semicircular blades mounted between two end plates. The investigated design of the Savonius rotor is characterized by the fact that the turbine shaft does not goes through the rotor. The main geometrical parameters of the wind turbine are shown in table 1. The principal scheme and the 3D model are presented on fig. 1. For the numerical modeling of the force interaction between the rotating wind rotor and the main flow the Sliding Mesh technique was adopted [3, 4]. The theoretical investigations are carried out at main flow velocity of $\upsilon_\infty = 20 \, m/s$.

The numerical modeling begins with the creation of a 2D geometrical model which is comprise by two separate areas. The first one is a circular rotating area in which the turbine is situated. The second one is a rectangular stationary area which represents the flow field around the turbine. The size of the computational domain and the applied boundary conditions are presented on fig. 2. The next step of the numerical procedure development is the generation of the computational mesh. For both computational areas an unstructured quadrilateral and triangular mesh is used. The accuracy of the solution greatly depends on the precise modeling of the laminar boundary sublayer in the near wall (blade) areas. In the area of the boundary layer a fine structural, quadrilateral mesh in used. The dimensionless criteria y^+ value reflects the quality and the influence of the near wall mesh over the turbulence model performance. This parameter characterizes the distance from the wall (blade) to the first computational node of the mesh. The y^+ value for the current study is $y^+ < 2.5$ at all operational regimes. The generated computational mesh is shown on fig. 3.
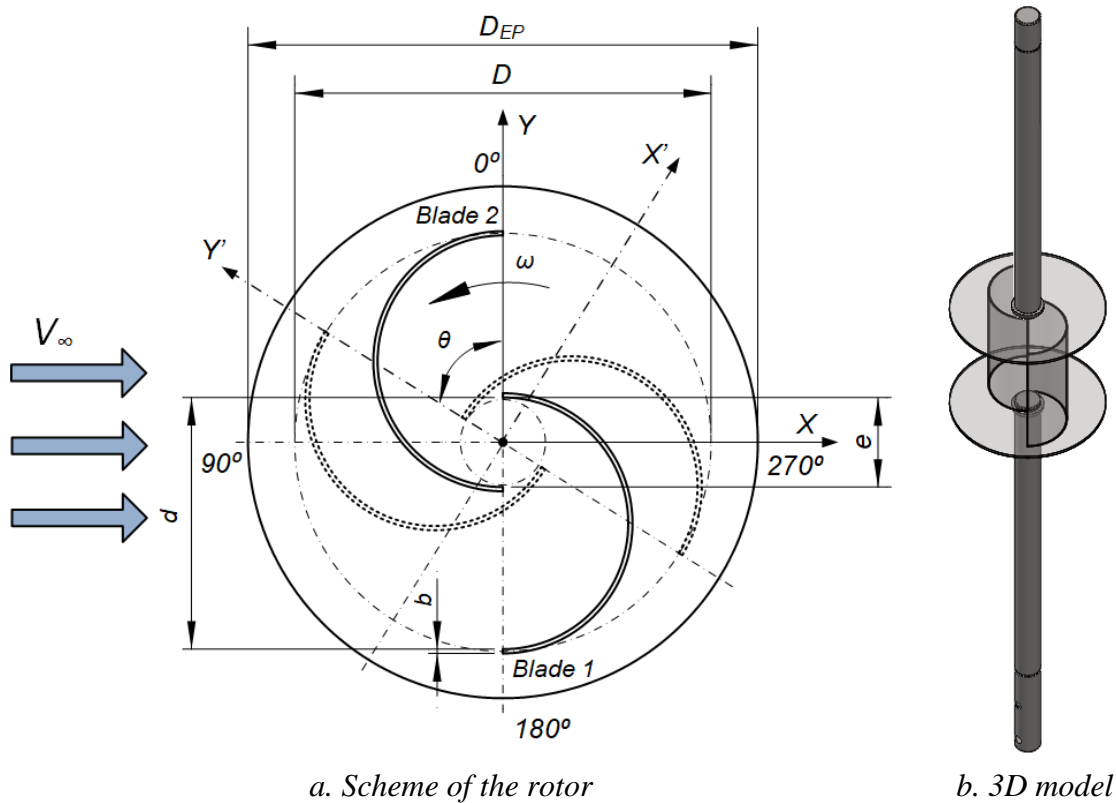
a. Scheme of the rotor   *b. 3D model*

Fig. 1 Principal scheme and 3D geometrical model

Table 1 Geometrical Parameters

Main geometrical parameters		
Diameter	**D**, m	0.1
Rotor High	**H,** m	0,1
Eccentricity	**e,** m	0.35
Number of Blades	**N**	2
Blade Thickness	**b,** m	0,001
End Plate Diameter	**D$_{EP}$**, m	0.03
Blade Diameter	**d**, m	0.06

The CFD software used in this study is ANSYS Fluent 14.0. Due to computational hardware and computational time limitations a 2D numerical study was conducted. The operation of the turbine is characterized by prominent unsteadiness of the flow passing through its rotor, due to which the Unsteady form of the Averaged Reynolds Navier-Stokes (URANS) equations was adopted. The formation and development of the turbulent structures is handled by the $k - \omega$ SST model [3]. A segregate scheme was used for the calculation of the discretized impulse equations in combination with the continuity equation. The SIMPLEC scheme was used to calculate the coupled pressure-velocity equations [3, 4]. For the time discretization a second order scheme was used. For the spatial discretization the PRESTO! scheme was applied for the pressure calculation. For all other variables a second order computational scheme was used.

The chosen value for the time-step size corresponds to the time for which the turbine rotates by *Δθ = 1°*. The numerical results were saved on every tenth time-step (*Δθ = 10°*) in order to reduce the volume of the accumulated computational data. The used number of inner iteration for the calculation of a single time step was 100.

Ahmedov et al. [2] carried out a numerical independence study over some of the computational parameters such as the mesh density, the number of rotor revolutions, the y^{+} criteria value etc., regarding a Savonius VAWT simulation. The numerical solver and computational mesh setup for the present study were done in accordance with Ahmedov et al. methodology.
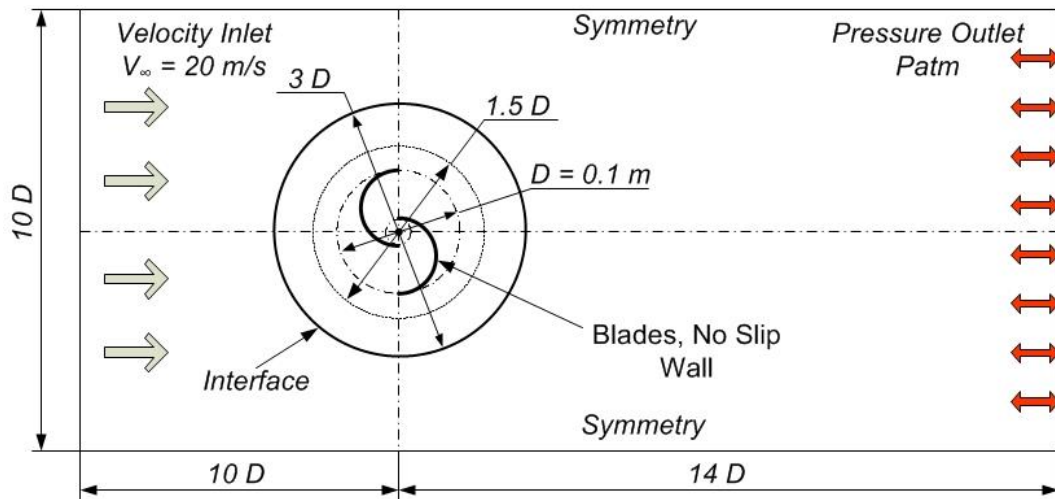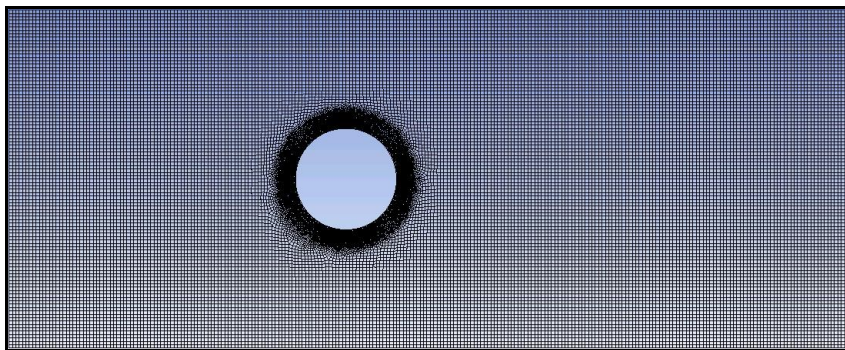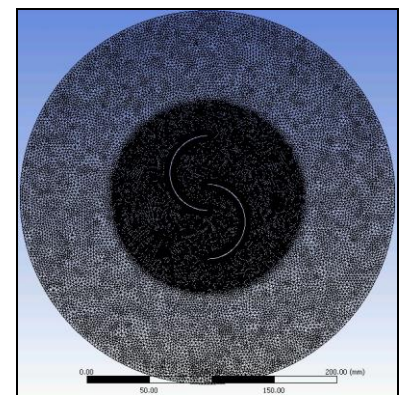
Fig. 2 Computational domain and boundary conditions

a. Stationary area   *b. Rotational area*

Fig. 3 Computational mesh at the stationary and rotational computational areas

Numerical Results

The main operational parameter of the Savonius wind turbine is the tip speed ratio (TSR) λ. This parameter depicts the ratio between the rotor peripheral velocity and the undisturbed main flow velocity. The TSR is given by

$$\lambda = \frac{u}{\upsilon_\infty},$$ (1)

where $u = \omega.R$ is the peripheral velocity of the rotor, R is the rotor radius, υ_∞ is the undisturbed main flow velocity.

The turbulence intensity fields for the range of angular positions $\theta = 0° \div 180°$ through interval of $\Delta\theta = 30°$ at TSR $\lambda = 0.125$, are shown on fig. 4 a. The rotor blades are interacting with continuously changing flow structures during the turbine operation. The initial positions of blade 1 and blade 2 is presented on fig. 1 a.

At angular positions at which the concave side of blade 1 is facing the main flow, there is no vortex generation on that surface. The generation and development of vortices strongly affects the pressure distribution on the blades surfaces. Massive vortex structures are forming and developing on blade 1 convex side. The attached massive structures are increasing the blade area, which leads to total pressure drop which is acting on the convex side of the blade. Blade 1 generates active torque at angular possessions perpendicular to the main flow.

The generated torque by blade 2 is reactive at angular positions of the rotor at which the blade convex side faces the main flow. But due to the hydrodynamic force generated by the secondary flow coming from the central rotor channel the reactive torque is overcome and even an active

torque is generated. The central rotor channel is formed by the overlapping of the two blades.

At operational regime characterized by TSR $\lambda = 0.125$ the generation, development and shading of large vortex structures is observed. As can be seen from the figure, at the convex side of the blades facing the main flow vortex structures are developing. These structures are disturbing the pressure distribution along the blade surface. This phenomenon is occurring during the blades passage through the rotor upstream area. The formation and detachment of vortex structures from the turbine rotor has a cyclical behavior. The behavior is alternating along the passage of the blades through the upstream area to the downstream area of the turbine rotor.

a. Turbulent Intensity at λ 0.125   *b. Turbulent Intensity at λ 0.5*
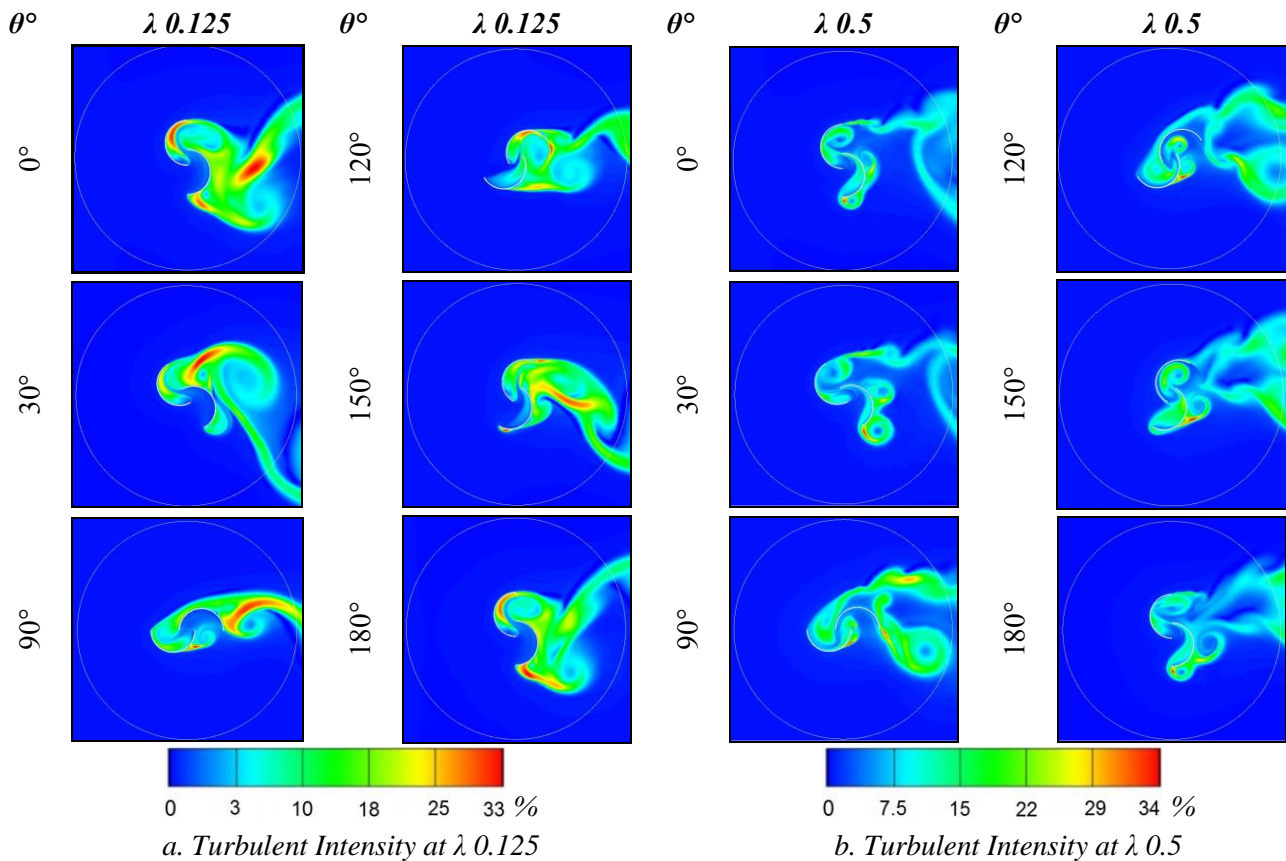
Fig. 4 Turbulent Intensity fields around the rotating wind turbine

The central rotor gap flow formed by the eccentric overlapping of the blades is the main factor which leads to vortex formation at the blades concave areas during the turbine rotation. The vortex structures developing behind blade 2 are result of the interaction between the central gap high velocity flow and the main flow. The central gap has a strong effect over the turbine performance under different operational regimes.

The turbulence intensity fields for the range of angular positions $\theta = 0° \div 180°$ through interval of $\Delta\theta = 30°$ at TSR $\lambda = 0.15$, are shown on fog. 4 b. At this operational regime the vortex generation at blade 2 concave surface and the large vortex development on blade 1 convex surface are presented. At this TSR the intensity of the vortex generation is less pronounced in comparison with TSR $\lambda = 0.125$. As can be seen from the figure the size of the generated and detached structures is smaller. The increase of the TSR is coupled with the increase of the wind turbine rotational speed. At these operational regimes the flow passing through the rotor is comparable with a flow passing around a cylinder. The turbulence intensity is diminishing which leads to the decrease of the aerodynamic drag of the wind rotor.

The dynamic variations of the vortex structures generation results in continually changing hydraulic losses during the turbine operation. These structures are the main factor causing disturbance of the pressure distribution along the blades surfaces. This unsteady operational

behavior results in fluctuations in the torque generation during the turbine rotation.
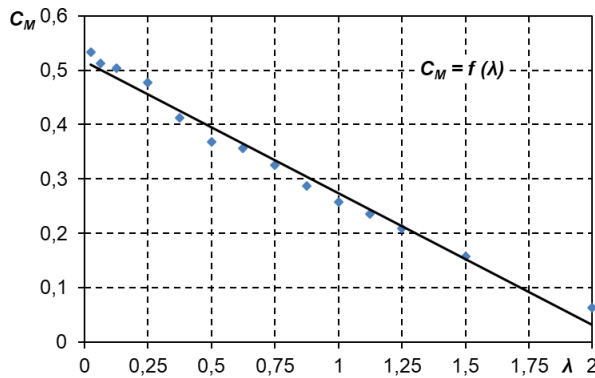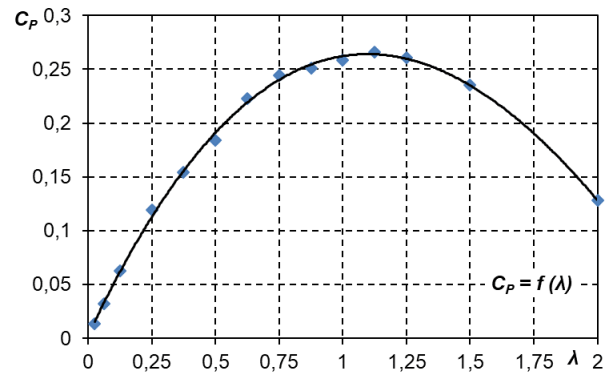
Fig. 5 Torque Coefficient	Fig. 6 Power Coefficient

The dimensionless torque and power coefficients are obtained through the following equations

$$C_m = \frac{M}{\rho \vartheta^2 R^2 H}, \tag{2}$$

$$C_P = \frac{P}{\rho \vartheta^3 RH}, \tag{3}$$

where ρ is the air density, H is the rotor height, M is the generated torque, P is the rotor output power.

The torque and power coefficients curves are shown on fig. 5 and fig. 6. As can be seen from fig. 5 the maximum of the characteristic falls into the area of low TSR. Whit the increase of the TSR the torque coefficient diminishes. The relation between the TSR and the torque coefficient values is well represented by a linear law.

The power coefficient as a function of the TSR is presented on fig. 6. The maximum of the power coefficient curve falls into a narrow operational region of TSR $\lambda = 0.75 \div 1.5$. The maximum value of the power coefficient is $C_P \approx 0.265$, reached at TSR $\lambda = 1.125$.

CONCLUSION

The flow field through the rotor was visualized at two different operational regimes characterized by TSR $\lambda = 0.125$ and $\lambda = 0.5$. At the low TSR, generation and separation of large vortex structures from the rotor's blades was observed. The generation of these large structures is primarily driven by the interaction of the main flow and the rotor central gap flow. With the increase of the TSR the turbulence intensity decreases. This is explained by the increase of the rotor angular velocity, which disrupts the central gap flow due to its high hydrodynamic resistance. Only the main flow interacts with the blades due to which the flow through the rotor resembles that of a flow over a cylinder.

The theoretical aerodynamic characteristic of the torque coefficient $C_m = f(\lambda)$ is approximated by a straight line with a negative slope. The absence of a maximum denotes the ability of the rotor to provide stable operation of the wind turbine (rotor coupled with drive machine) regardless to the dynamic changes of the operational load.

The operational regimes at which the wind rotor has high power coefficient of around $C_P \approx 0.265$ falls into a narrow area of tip speed ratios $\lambda = 0.75 \div 1.5$. This has to be considered when coupling the wind rotor with the drive machine (electrical generator, water pump etc.) in order for suitable transmission ratio of the mechanical gear to be selected.

REFERENCES

[1] Abraham J. P., Mowry G. S., Plourde B. P., Sparrow E. M., Minkowycz W. J. *Numerical simulation of fluid flow around avertical-axis turbine*. Journal of Renewable and Sustainable Energy 2011; 3 (3): 1–13.

[2] Ahmedov A., Tujarov K., Popov G. *Methodology for Numerical Modelling the Performance of Vertical Axis Wind Turbines*. In: University of Ruse Proceedings volume 53, book 1.2, Heat transfer, hydraulic and pneumatic engineering. Ecology and environmental protection. Design and ergonomics, Ruse 2014, ISBN 1311-3321.

[3] ANSYS Fluent 14.0, *Theory Guide*.

[4] ANSYS Fluent 14.0, *User Guide*.

[5] Jaohindy P., Ennamiri H., Garde F., Bastide A. *Numerical investigation of airflow through a Savonius rotor*. Wind Energy 2013.

[6] Launder B. E., Spalding D. B. *The numerical computation of turbulent flo*ws. Computer Methods in Applied Mechanics and Engineering 1974; 3 (2):269–89.

[7] Menter F. R. *Two-equation eddy-viscosity turbulence models for engineering applications*. AIAA Journal 1994; 32(8): 1598–605.

[8] Menter F. R. *Zonal two-equation k–ω turbulence models for aerodynamic flows*. In Proceedings of the 24th AIAA Fluid Dynamics Conference, Orlando, FL; 6–9 July 1993.

[9] Plourde B. D., Abraham J. P., Mowry G. S. *Simulations of three-dimensional vertical axis turbines for communication applications*. Wind Engineering 2012;36 (4): 443–54.

[10] Pope K., Rodrigues V., Doyle R., Tsopelas A., Gravelsins R., Naterer G. F., et al. *Effects of stator vanes on power coefficients of a zephyr vertical axis wind turbine*. Renewable Energy 2010; 35(5):1043 – 51.